Displacement Measurement of Soft Material Indentation using Light Intensity

Mohd Nadzeri Omar, Mohd Hasnun Arif Hassan*
Faculty of Mechanical and Automotive Engineering Technology,
Universiti Malaysia Pahang, 26600 Pekan, Pahang
*nadzeri@ump.edu.my

ABSTRACT

This paper studies proof of concept in which soft material displacement during indentation is measured by a change in light intensity as the indenter is pushed into a soft material. The Light Dependent Resistor (LDR) sensor, which is embedded within a transparent hemispheric indenter, is used to measure the intensity of light while the indenter is on the surface and within the soft material. The change in light intensity contributes to a gradient that can be used to calculate the displacement of the soft material. The calculated difference in light intensity is converted into a displacement with the mean conversion factor obtained from the calibration equation. Measurements were carried out on three silicone samples with varying elastic properties over a range of different light intensities. By referring to linear regression and R-squared values, the proposed concept has high consistency in measuring the difference of light intensity for various materials at different initial light intensities with more than 95% of R-squared values. In addition, the mean of variance between measurements, reflecting repeatability, is within an outstanding 1.5%. In the meantime, the accuracy of the proposed concept tested concerning the actual displacement is less than 10% of the variation. With promising results, the proposed design can be applied as a standalone technology or as an extension to a hand-held soft material characterization device for further improvement.

Keywords: *Displacement Measurement; Light-dependent Resistor; Indentation; Soft Material Deformation*

Mohd Nadzeri Omar, Mohd Hasnun Arif Hassan

Introduction

Characterization of soft materials, especially soft tissues, plays a significant role in biomedical applications. In the case of breast cancer, the elasticity characterization is used to differentiate between healthy and unhealthy tissues. For the past few decades, the characterization process has been carried out using a clinical breast examination machine. During the process, the target tissue will be exposed to a variety of actuating elements to regulate the deformation. The tissue elasticity is then retrieved from the deformation result. The approach, however, has disadvantages, such as the characterization process which can only be conducted by experienced clinicians, resulting in higher clinical costs and time-consuming. In addition, the availability of the machine is still limited and thus prevents early detection, which may be devastating for cancer patients [1]. Several studies have recently been conducted to provide a compact, inexpensive, and accurate self-characterization device [2]-[5]. With such a device, early screening can be performed on a personal basis and avoids an awkward feeling [6].

As the soft material characterization can be made from the elasticity measurement, force and displacement are the two important parameters to be considered when evaluating the elasticity [7][8]. This paper focuses on the calculation of the second parameter that is the displacement during deformation.

Displacement Measurement

Sahu et al. [9] applied a visual inspection using an optical camera and a hyperspectral imaging sensor to observe the transverse displacement of the lesion. However, when the camera is used, the privacy of the patient can become a concern. On top of that, the unit can be bulky with the attachment of certain instruments.

The rapid development of the strain gauge includes a variety of strain gauges, including the application to measure the displacement of the lesion. The strain gauge is usually connected to a beam, such as a cantilever beam, where the deflection of the beam is converted into the strain measure [10][11]. A small gap is needed to allow the beam to be deflected. However, some particles, such as debris or fluid, may fill the gap and affect the measurement.

The fibre optic sensor is another type of sensor used in the displacement measurement [12]-[16]. Optical-based sensors have many advantages over strain gauges, such as high feedback rate and sensitivity [10][17][18]. Puangmali et al. [17] used a single fibre optic to transmit light source to a reflector that is attached to the deformation tip, and the reflected light is captured by another fibre optic sensor before being analysed by a

photodetector. The efficiency of the mechanism on the uneven surface is, however, poor. Liu et al. [19] added three pairs of transmitters and receiver fibres to allow stable measurements on uneven surfaces, but errors still occurred due to inconsistent transmitted light caused by the drift of transmitted light and dust particles on the reflector, which can degrade the reflected light [17].

Hampson et al. [3] used the acceleration sensor to calculate the acceleration of the characterization probe, which was then incorporated for displacement readings. Although the recorded results showed a high accuracy of 4% of the variance with the industrial universal testing unit, the application required the user to apply the device at a certain angle to allow an accurate measurement of the acceleration. Since dual integration was used, an error occurred due to quadratic drift in the measured displacement.

Indentation is a well-used method for quantifying the mechanical properties of a material. In the case of a soft material indentation, the soft material is displaced at the point of contact according to the depth travelled by the indenter. When the indenter travels through the soft material, the light that hits the tip of the indenter is reduced. The change in light intensity contributes to a gradient that can be used to calculate the material displacement. With the analogy, an alternative approach for calculating displacement is suggested using the Light Dependent Resistor (LDR) sensor.

The LDR sensor has been used in a wide range of applications. For example, Nasrudin et al. [20] used the LDR sensor to control the motion of their automated robot. In the study, the LDR sensor was coupled with a super bright LED as a light source. On the other hand, Dadi et al. [21] used the LDR sensor to guide the movement of their solar panels. In the study, ambient light was used as a source of light. The two studies showed the ability of an LDR sensor to determine light intensity either in a controlled or in an ambient light condition.
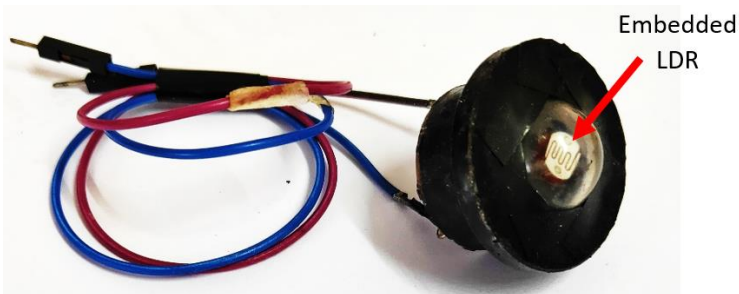
Figure 1: The image of the hemispheric transparent indenter with the LDR sensor inside it.

Methodology

Measurement components

The proposed concept consists of the NOPRS-12 Light Dependent Resistor (LDR) sensor (Advance Phototonix Inc., USA) and the Arduino Nano ATmega328 microcontroller board (Microchip Technology Inc., USA).

A transparent indenter was produced using a transparent epoxy resin. The liquid mixture of the epoxy resin and the hardener, at a weight ratio of 3:1, was poured into a silicone mould to form the indenter. The indenter had a hemispheric tip of 15 mm in diameter and was connected to a 32 mm circular guard which was used to isolate the excess force beyond the maximum indenter displacement of 7.5 mm. The LDR sensor was embedded within the hemispheric tip, with the light-collecting surface facing the subject material. Other surfaces, except the hemispheric surface, were painted dark to prevent light from reaching the LDR sensor from other directions. The LDR sensor was attached to the Arduino Nano board by two extension wires (see Figure 1). Power was supplied to the Arduino Nano board by a Universal Serial Bus (USB) port that was also used to connect the sensor and the device. The measured data were transmitted to the machine at a rate of 9.6 kHz without any buffering.
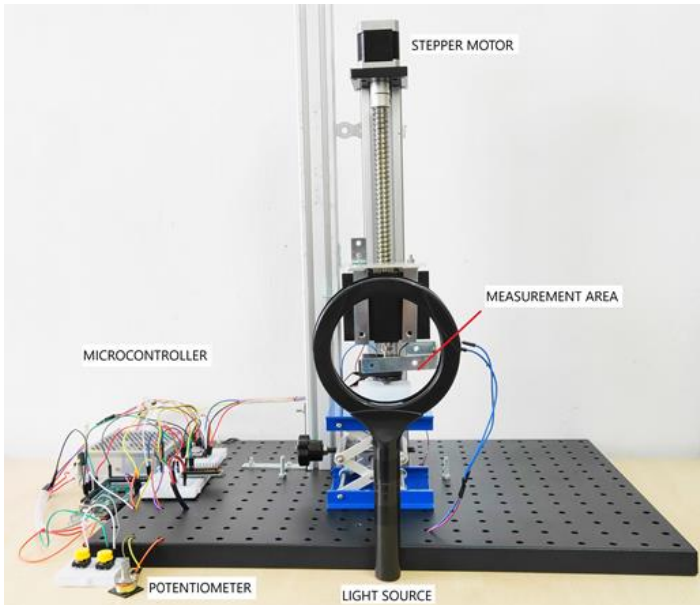
Figure 2: The automated handling system used in the experimental setup.

Experimental setup

The experimental setup is as shown in Figure 2. The indenter is held loosely by a circular grip mounted on a fixed extension bar. This allows the indenter to travel freely in a vertical direction only.

An extension rod with a circular tip was mounted on a linear guide rail powered by the NEMA 17HS4401 Bipolar Stepper Motor with a resolution of 200 steps or 5 mm per revolution. The stepper motor, which was regulated by the Arduino Mega 2560 R3 microcontroller board (Microchip Technology Inc., USA), moved the extension rod vertically onto the indenter and pushed the indenter towards the subject material placed on a lifting platform.

LED light was used to provide additional light to the measurement area. The LED light was mounted on an external handle, placed 15 mm from the sample. The LED light intensity was adjusted by a potentiometer connected to the same Arduino Mega 2560 R3 board.

Test materials

Instead of using a real soft tissue sample, silicone mixtures were used as a test material at this point. The silicone samples used in this study were formed using the Ecoflex 00-30 series (Smooth-on Inc., USA), which resemble human soft tissue [22].

Three silicone samples with different elastic values were formed by mixing different ratio mixtures of two elastomer components, A and B, which are 1:1, 2:1, and 3:1, respectively. The silicone samples were shaped into a rectangular cube with a length of 50 mm, a width of 45 mm, and a depth of 20 mm.

The elasticity of the samples was determined using the Instron 3342 industrial universal testing machine (Instron Engineering Corp., UK). In this process, the silicone samples were compressed to 5 mm, which was about 25% of the strain. The resulting elasticity is shown in Table 1.

Table 1: Elasticity of the silicone samples

Sample	Elasticity (MPa)
A	0.232
B	0.241
C	0.289

Data collection

The transparent indenter with the LDR sensor inside was pushed vertically onto the silicone sample by the extension rod at a speed of 2.5 mm/s at a constant travel distance of 4.5 mm. The constant distance of travel was

accomplished by controlling the steps of the stepper motor. The stepper motor was set to drive 180 steps, which was equal to 4.5 mm.
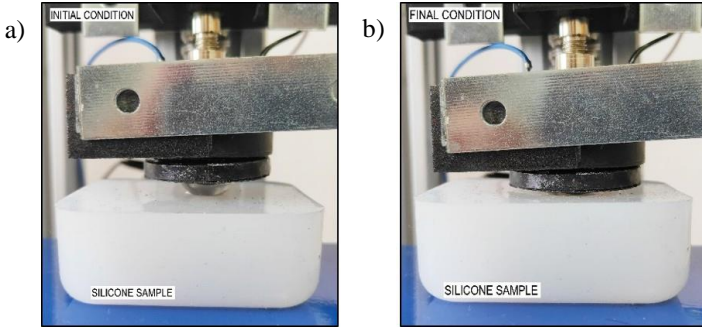
Figure 3: The image of the indenter with the LDR sensor in two conditions. a) The initial condition where the indenter is located on the surface of the silicone sample, and b) Final condition where the indenter has moved 4.5 mm into the silicone sample.

Two sets of data were obtained, which are the initial light intensity and the light intensity, when the indenter travelled 4.5 mm into the silicone sample as seen in Figure 3. Both data sets were recorded for a few seconds. The mean value of the recorded data was calculated to reflect a single light intensity value at each condition. The calculation was repeated ten times for a range of three samples of silicone and several initial light intensities. The light intensity for one measurement cycle at three different initial light intensities is shown in Figure 4, which highlights the position of the sensor.

Based on the collected data, the difference in light intensity was calculated. The difference in light intensity represents the displacement of the sample. A conversion process is required to convert the difference in light intensity into displacement. With a known travelled distance of 4.5 mm, in this case, a conversion factor, x, that can be used to convert the difference in light intensity into millimetres can be measured using Equation (1).

$$x = \frac{\alpha}{\beta} \tag{1}$$

where α is the known displacement and β is the measured difference in light intensity.
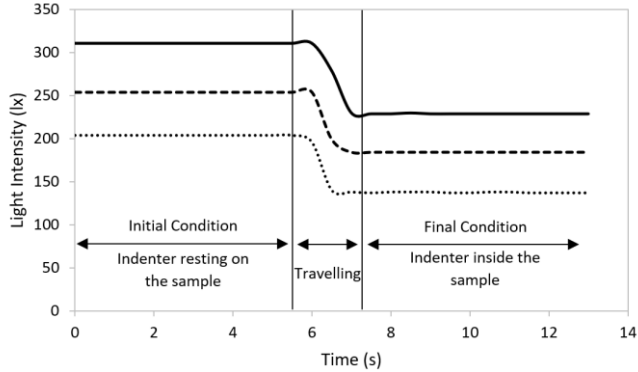
Figure 4: Graphic representation of the initial and final indentation showing the light intensity concerning time over a single cycle of measurement.

Results

Figure 5 shows the mean value of the difference in light intensity at different initial light intensities for the three silicone samples. The calculated data are then plotted individually in Figure 6 for each silicone sample to study the individual behaviour of the proposed concept. Linear regression with an R-squared value is demonstrated.
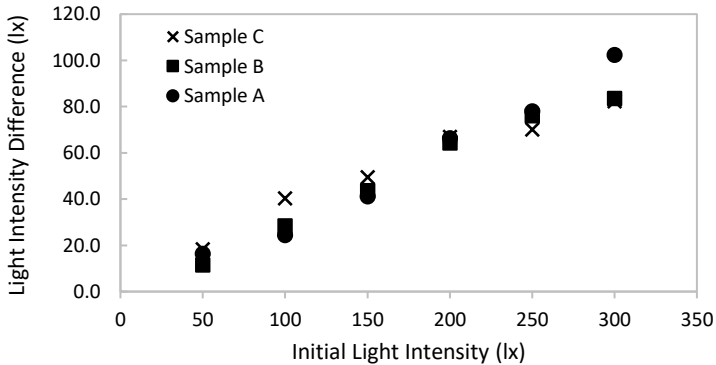
Figure 5: Mean values of light intensity difference recorded at different initial light intensities over the three silicone samples.
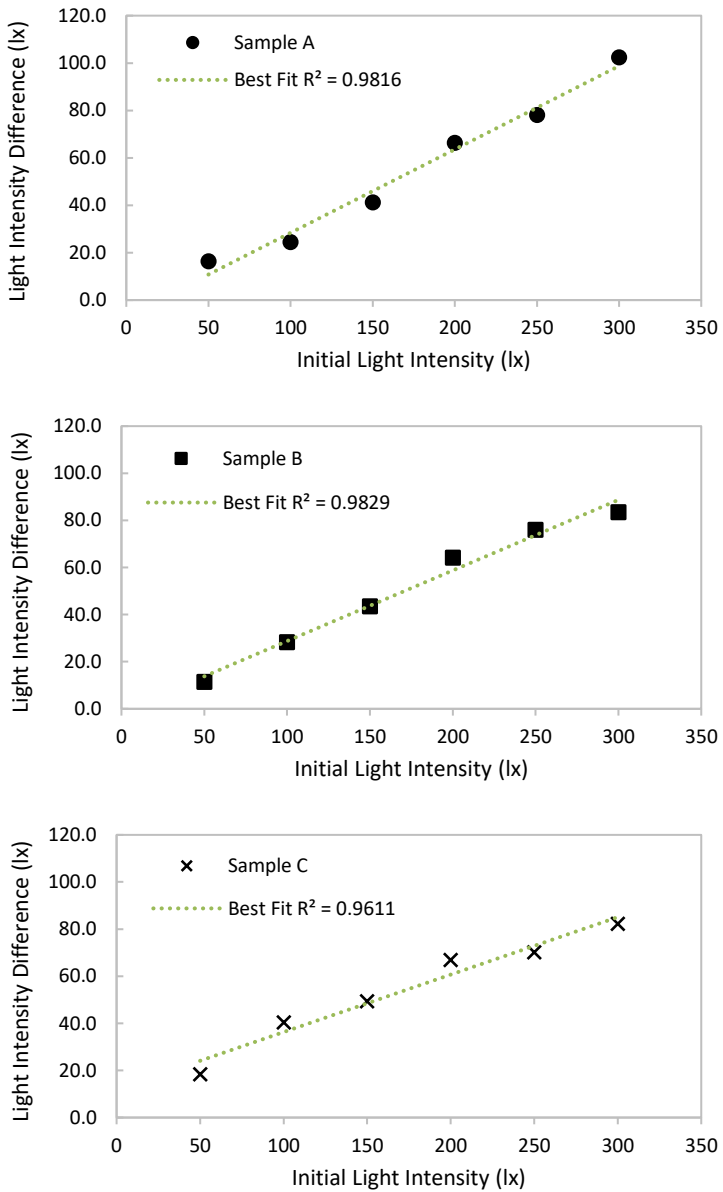
Figure 6: Individual plot of light intensity difference versus initial light intensities over the three silicone samples.
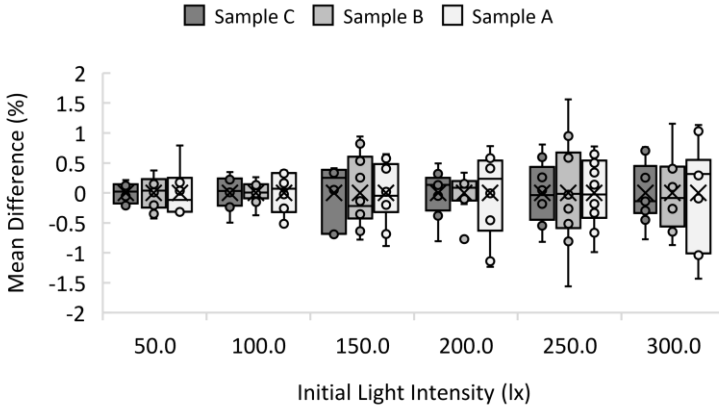
Figure 7: The box plot of the mean difference percentage for all silicone samples at various initial light intensities.

Table 2: Repeatability evaluation

Cycle	Test 1 (lx)	Test 2 (lx)	Test 3 (lx)
1	68.307	69.538	69.850
2	69.231	69.714	69.774
3	68.594	70.043	70.354
4	69.295	69.313	69.063
5	69.214	69.697	69.579
6	69.044	69.228	69.133
7	69.305	69.401	69.521
8	68.643	69.917	69.049
9	68.893	69.958	69.282
10	68.986	69.292	69.647
Mean measurement (lx)	69.362		
Largest measurement variance	1.055 (1.5%)		
Lowest measurement variance	0.992 (1.4%)		

Two methods were used to test the repeatability of the proposed concept. First, it was measured by calculating the mean difference between measurements at different initial light intensities over the three silicone samples. The results are plotted in Figure 7. For the second method, the repeatability was determined by the repeated analysis of the same sample and initial light intensity. Here, both the sample (Sample 2) and the initial light

intensity (200 lx) were selected at random. The measurement was repeated at a time interval between 1 - 3 mins, to allow the sample to return to its original shape before the next analysis. The findings are shown in Table 2.

Table 3: Accuracy evaluation of the proposed concept. The conversion factors calculated at three displacement values are compared and the mean conversion factor is used to convert the difference in light intensity into the displacement value

Initial light intensity (lx)		200	
Displacement (mm)	2.0 (80 steps)	3.0 (120 steps)	4.0 (160 steps)
Mean light intensity difference (lx)	14.55	24.16	32.99
Conversion factor	0.137	0.124	0.121
Mean conversion factor		0.128	
Variance in conversion factor	-0.01 (8%)	0.003 (2%)	0.006 (5%)
Calibrated displacement value using the mean conversion factor (mm)	1.857	3.083	4.21
Variance of the calibrated displacement with the exact displacement value (mm)	-0.143 (7%)	0.083 (3%)	0.21 (5%)

The accuracy of the proposed concept depends on the conversion factor. Theoretically, the conversion factor should be the same in a controlled identical setting. Table 3 shows the evaluation of the conversion factor at three displacement points. The three displacement points are achieved by controlling the steps of the stepper motor. Based on the calculated conversion factors, the mean values are determined and the measured difference in light intensity is converted into displacement using the mean conversion factor. The accuracy of the proposed concept is assessed by determining the variation between the converted displacement and the actual displacement values. The variation is shown in Table 3.

Table 4: Repeatability evaluation of the percentage of difference in light intensity measured at various initial light intensities on the three silicone samples

Initial Light Intensity (lx)	Average Difference (lx)	Percentage Difference (%)
Sample A		
50	18.3	36.6
100	40.3	40.3
150	49.4	32.9
200	66.9	33.5
250	70.1	28.1
300	82.3	27.4
Sample B		
50	11.4	22.9
100	27.4	28.4
150	43.6	29.1
200	64.3	32.1
250	76.1	30.4
300	83.6	27.9
Sample C		
50	16.4	32.8
100	24.4	24.4
150	41.1	27.4
200	66.3	33.2
250	78.0	31.2
300	102.4	34.1
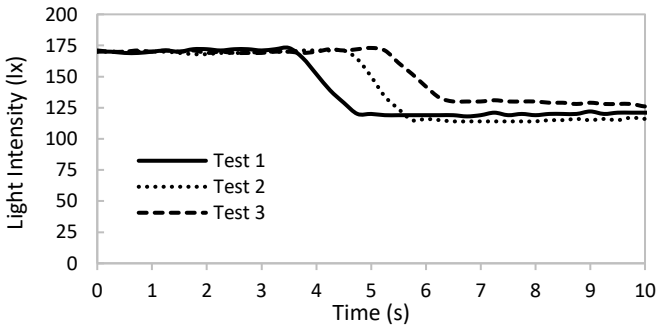
Figure 8: Three measurement cycles are taken with ambient light. Although the initial light intensity is identical, different final light intensities are recorded.

Discussion

Light intensity results

Figure 5 demonstrates the initial light intensity that plays a major role in the measurement process. While the distance travelled by the indenter is constant at each initial light intensity, the difference in the measured light intensity varies. The difference in light intensity is relative to the initial light intensity, which suggests a greater difference in light intensity at a high initial light intensity. However, when looking at the percentage of the difference in light intensity over the initial light intensity, the value ranges from 20% to 40%, as seen in Table 4. While variations throughout the difference in light intensity have been seen, concerning its initial light intensity, only a minor deviation is observed. It suggests that a similar reduction percentage can be measured at any initial light intensity that provides the same travelled distance.

In addition, Table 4 brings up another question on how to find the best measuring condition. Some factors need to be considered. First, the availability of light intensity. For a lower light intensity level, the sensor must be concealed from the ambient light intensity. In this case, for example, the sensor can be mounted within an opaque housing. However, it is very difficult to monitor the ambient light as it involves a variety of influences, such as reflections and shadings [20, 23]. As shown in Figure 8, measurements are not consistent when taken at ambient light, even if the initial light intensity is the same. Dadi et al. have also highlighted the similar problem [21]. Alternatively, external lighting can be used to provide additional illumination to the measurement area. External lighting has been used widely in optic-based applications such as reported in Arabzadeh et al. [24] and Khamis et al. [25]. In both studies, LEDs were used to generate the light and were placed close to optic sensors. The presence of external lighting can provide an evenly distributed illumination. On top of that, Durig et al. [26] suggest that the measurement should be taken in the absence of the fluorescent light due to the interference that it can generate. During et al. recommend the best condition for the measurement is in the dark.

The conversion factor is another element to be considered. The conversion factor is required to convert the difference in measured light intensity to displacement. Based on Equation (1), a larger difference in light intensity is preferable as it results in a smaller conversion factor. The sensitivity of the proposed concept would be higher with a smaller conversion factor.

Linear regression results

The linear regression line plotted in Figure 6 shows the behaviour of the proposed concept over different light intensities. The regression line refers to the expected difference in light intensity at any initial light intensity. From the

regression line, the R-squared value indicates how close the real value is to the expected value. It can be observed that the R-squared values for all silicone samples are more than 96%. It implies that the difference in light intensity at any initial light intensity can be predicted with high precision [3]. The results demonstrate a high consistency of the proposed concept.
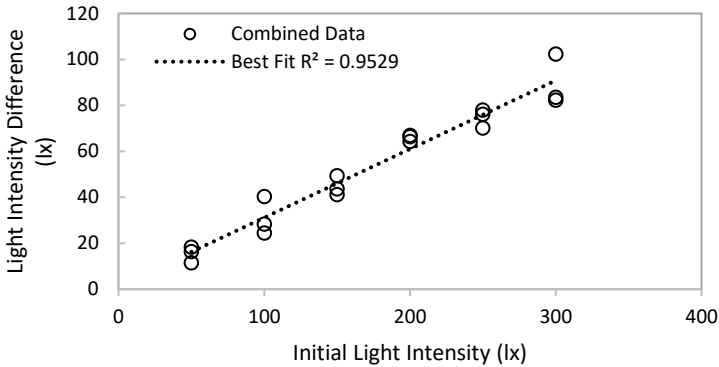
Figure 9: Combination of measured data for all silicone samples to determine linear regression with relation to different materials.

As seen in Table 1, the three silicone samples used in this analysis have different elastic values. It is also essential to note the consistency of the proposed concept over different materials. The data used in Figure 5 have been combined to find a linear regression line and its R-squared value. As shown in Figure 9, the R-squared value is more than 95%. Thus, it suggests that the proposed definition can be applied to materials with elastic value in the range of 200 to 300 kPa which is a common range for lump in breast cancer [27].

Repeatability results
Figure 7 demonstrates excellent repeatability for all samples and initial light intensities. It suggests the reliability of the measurement methodology as it has achieved repeatability on raw data without any statistical outlier rejection being applied. The individual repeatability of the sample determines the overall system repeatability, and when the mean response is considered, as shown in Figure 7, the variation in repeatability is less than 1.5%. In addition, as shown in Table 2, when repeated measurements are performed on the same sample, the variance of each measurement concerning the mean value is less than 2%, which is similar to the performance obtained by Hampson et al. [3]. With excellent repeatability, the proposed method overcomes the repeatability limitation of the existing palpation methods especially those with light intensity modulated (LIM)-based [28].

Accuracy

The crucial part of the proposed concept is to convert the difference in measured light intensity into displacement. The conversion process can be conveniently carried out by using a conversion factor of Equation (1). The accuracy of the proposed concept is therefore dictated by the conversion factor. As shown in Table 3, the conversion factors calculated at the three displacement points are different. Their mean value is determined to quantify the difference. By using the mean value, the difference in the measured light intensity is converted into displacement. The accuracy is then assessed by measuring the variance of the converted displacement concerning the actual displacement. It can be shown that the overall difference is less than 10%. Although the 10% variation is small enough, the sensitivity of the proposed concept needs to be enhanced for material characterization applications where a small shift in displacement is significant [15]. On the other hand, the actual displacement value is obtained by assuming that the stepper motor has accurately generated that amount of displacement [29, 30]. However, the value may be different. If the accuracy of the stepper motor is considered, the measured variation can be smaller.

Limitations

There are some drawbacks to the present proof of concept setup. First, the additional light used to illuminate the measurement area is isolated and placed at a distance from the measurement area. While reliable results are obtained, the light comes from one source, and it is possible for shadows to occur and to influence the measurement. Future studies should be conducted to identify the type and best place to locate additional light so that consistent lighting can be added [31].

The second drawback of the original setup is that the movement of the indenter is regulated by an electrical actuator renowned for its precision. In the case of a human-handled indenter, the movement of the indenter may not be perfectly vertical and may result in inconsistent compression. The same limitation is highlighted in other handheld devices [3, 5, 32]. Specific mechanisms for removing the error must be implemented when translating the proposed concept into a product.

For the proposed concept to operate properly, the indenter must be completely submerged in the sample. To do this, the material properties of the sample under investigation are important [8]. For example, the proposed concept cannot be applied to dense materials such as bone. It is therefore important to define the operating range of the system, particularly in terms of elasticity. In this analysis, only three material samples are used, which are inadequate to study the operating range. Further analysis can be done by having more samples to determine the operating range [22].

Conclusion

This paper presents an alternative concept in determining the displacement of soft materials during the indentation process. The proposed concept uses a Light Dependent Resistor (LDR) embedded within a transparent hemispheric indenter to calculate the difference in light intensity during the process. The calculated light intensity difference is then converted to a displacement value with the mean conversion factor obtained from the calibration equation.

Measurements are carried out on three silicone samples with different elastic values and replicated at different initial light intensities. It is found that the proposed definition has a very good consistency concerning various materials and light intensities, with R-squared values of more than 95% in both cases. The repeatability of the proposed definition is quantified by the variation between measurements. The proposed concept has achieved very strong repeatability, with a variation of 1.5% for each measurement at various materials and light intensities.

As far as accuracy is concerned, the proposed concept can evaluate a soft material displacement with a maximum deviation of less than 10%. Despite the small variance, the accuracy of the proposed concept needs to be improved because the displacement value is crucial in material characterization.

With further enhancements, the proposed concept can provide a cheaper, compact, and accurate alternative to calculate the displacement of compressed soft material. Soon, it can be used in a portable application for material characterization, such as an early screening device for cancer lesions.

Acknowledgement

References

[1] N. D. Nik Farid, N. Abdul Aziz, N. Al-Sadat, M. Jamaludin, and M. Dahlui, "Clinical Breast Examination As the Recommended Breast Cancer Screening Modality in a Rural Community in Malaysia; What Are the Factors That Could Enhance Its Uptake?," *PLoS ONE*, vol. 9, no. 9, pp. 1-6, 2014.

[2] R. B. Broach, R. Geha, B. S. Englander, L. DeLaCruz, H. Thrash, and A. D. Brooks, "A cost-effective handheld breast scanner for use in low-resource environments: a validation study," *World Journal of Surgical*

Oncology, vol. 14, no. 1, pp. 2-6, 2016.

[3] R. Hampson, G. Dobie, and G. West, "Elasticity Measurement of Soft Tissues Using Hybrid Tactile and MARG-Based Displacement Sensor Systems," *IEEE Sensors Journal*, vol. 19, no. 22, pp. 10262–10270, 2019.

[4] C. Li, G. Lü, and J. Shen, "Tactile sensor with an inverted V-shaped indenter for elastic tissue identification," *Intelligent Service Robotics*, vol. 13, no. 1, pp. 113–121, 2019.

[5] P. Peng and R. Rajamani, "Handheld Microtactile Sensor for Elasticity Measurement," *IEEE Sensors Journal*, vol. 11, no. 9, pp. 1935–1942, 2011.

[6] E. L. Cohen, B. R. Wilson, R. C. Vanderpool, and T. Collins, "Identifying Sociocultural Barriers to Mammography Adherence Among Appalachian Kentucky Women," *Health Communication*, vol. 31, no. 1, pp. 72–82, 2015.

[7] A. B., S. Rao, and H. J. Pandya, "Engineering approaches for characterizing soft tissue mechanical properties: A review," *Clinical Biomechanics*, vol. 69, pp. 127–140, 2019.

[8] T. D. Nagy and T. Haidegger, "Recent Advances in Robot-Assisted Surgery: Soft Tissue Contact Identification," *2019 IEEE 13th International Symposium on Applied Computational Intelligence and Informatics (SACI)*, 2019.

[9] A. Sahu, F. Saleheen, V. Oleksyuk, Y. Chen, and C.-H. Won, "Tactile and hyperspectral imaging sensors for mammary tumor characterization," 2013 *IEEE Sensors*, pp. 1-4, 2013.

[10] S. V. Beekmans, D. Iannuzzi, and J. J. van den Dobbelsteen, "Characterizing tissue stiffness at the tip of a rigid needle using an opto-mechanical force sensor," *Optical Elastography and Tissue Biomechanics III*, pp. 1-8, 2016.

[11] L. Zhang, F. Ju, Y. Cao, Y. Wang, and B. Chen, "A tactile sensor for measuring hardness of soft tissue with applications to minimally invasive surgery," *Sensors and Actuators A: Physical*, vol. 266, pp. 197–204, 2017.

[12] Y. Tanaka, M. Nemoto, and Y. Yamada, "Displacement measurement Using Two-photon Absorption process IN Si-Avalanche photodiode and Fiber BRAGG GRATINGS," *Journal of Lightwave Technology*, vol. 36, no. 4, pp. 1192–1196, 2018.

[13] P.-J. Chen, Z.-R. Yu, J.-H. Wang, Y.-H. Lin, W.-J. Peng, H.-L. Chen, W.-Y. Hsu, C.-Y. Chan, and C.-H. Hwang, "Development of active displacement detector for slight vibration measurement," *2018 IEEE International Instrumentation and Measurement Technology Conference (I2MTC)*, pp. 1-6, 2018.

[14] H. Khamis, B. Xia, and S. J. Redmond, "A novel optical 3D force and displacement sensor – Towards instrumenting the PapillArray tactile sensor," *Sensors and Actuators A: Physical*, vol. 291, pp. 174–187, 2019.

[15] A. Suebsomran, "Design and control of a passive compliant actuation with positioning measurement by LED and photodiode detector for medical application," *Measurement and Control*, pp. 1–15, 2021.

[16] T. Nuntakulkaisak, Y. Infahsaeng, R. Bavontaweepanya, and E. Pongophas, "The signal calibration from a Sagnac polarized standing wave interferometer for displacement measurement," *Journal of Physics: Conference Series*, vol. 1719, no. 1, p. 012047, 2021.

[17] P. Puangmali, H. Liu, K. Althoefer, and L. D. Seneviratne, "Optical Fiber Sensor for Soft Tissue Investigation during Minimally Invasive Surgery," *2008 IEEE International Conference on Robotics and Automation*, pp. 2934-2939, 2008.

[18] D. Zbyszewski, P. Polygerinos, L. D. Seneviratne, and K. Althoefer, "A novel MRI compatible air-cushion tactile sensor for Minimally Invasive Surgery," 2009 IEEE/RSJ International Conference on Intelligent Robots and Systems, pp. 2647-2652, 2009.

[19] H. Liu, P. Puangmali, D. Zbyszewski, O. Elhage, P. Dasgupta, J. S. Dai, L. Seneviratne, and K. Althoefer, "An indentation depth—force sensing wheeled probe for abnormality identification during minimally invasive surgery," *Proceedings of the Institution of Mechanical Engineers, Part H: Journal of Engineering in Medicine*, vol. 224, no. 6, pp. 751–763, 2010.

[20] V. Dadi and S. Peravali, "Optimization of light-dependent resistor sensor for the application of solar energy tracking system," *SN Applied Sciences*, vol. 2, no. 9, pp. 1-13, 2020.

[21] N. Nasrudin, N. M. Ilis, T. P. Juin, T. T. Chun, L. W. Zhe, and F. Z. Rokhani, "Analysis of the light dependent resistor configuration for line tracking robot application," *2011 IEEE 7th International Colloquium on Signal Processing and its Applications*, pp. 500-502, 2011.

[22] J. L. Sparks, N. A. Vavalle, K. E. Kasting, B. Long, M. L. Tanaka, P. A. Sanger, K. Schnell, and T. A. Conner-Kerr, "Use of Silicone Materials to Simulate Tissue Biomechanics as Related to Deep Tissue Injury," Advances in Skin & Wound Care, vol. 28, no. 2, pp. 59–68, 2015.

[23] M. Carrasco, A. Laudani, G. Lozito, F. Mancilla-David, F. Riganti Fulginei, and A. Salvini, "Low-Cost solar Irradiance sensing for PV Systems," *Energies*, vol. 10, no. 7, pp. 998, 2017.

[24] E. Arabzadeh, E. Zorzin, and M. E. Diamond, "Neuronal encoding of texture in the Whisker Sensory Pathway," *PLoS Biology*, vol. 3, no. 1, pp. e17, 2005.

[25] H. Khamis, B. Xia, and S. J. Redmond, "A novel optical 3D force and displacement sensor – Towards instrumenting the PapillArray tactile sensor," *Sensors and Actuators A: Physical*, vol. 291, pp. 174–187, 2019.

[26] F. Dürig, A. L. Albarracín, F. D. Farfán, and C. J. Felice, "Design and construction of a photoresistive sensor for monitoring the rat vibrissal displacement," *Journal of Neuroscience Methods*, vol. 180, no. 1, pp. 71–

76, 2009.

[27] L. Zhang, F. Ju, Y. Cao, Y. Wang, and B. Chen, "A tactile sensor for measuring hardness of soft tissue with applications to minimally invasive surgery," *Sensors and Actuators A: Physical*, vol. 266, pp. 197–204, 2017.

[28] C. Lv, S. Wang, and C. Shi, "A High-Precision and Miniature Fiber Bragg Grating-Based Force Sensor for Tissue Palpation During Minimally Invasive Surgery," *Annals of Biomedical Engineering*, vol. 48, no. 2, pp. 669–681, 2019.

[29] G. Baluta and M. Coteata, "Precision microstepping system for bipolar stepper motor control," *2007 International Aegean Conference on Electrical Machines and Power Electronics*, pp. 291–296, 2007.

[30] L. Zhang, L. Liu, J. Shen, J. Lai, K. Wu, Z. Zhang, and J. Liu, "Research on stepper MOTOR motion control based on MCU," *2017 Chinese Automation Congress (CAC)*, pp. 3122–3125, 2017.

[31] B. Prabowo, A. Purwidyantri, and K.-C. Liu, "Surface plasmon Resonance Optical Sensor: A review on light source technology," *Biosensors*, vol. 8, no. 3, pp. 2-27, 2018.

[32] P. Schiavone, F. Chassat, T. Boudou, E. Promayon, F. Valdivia, and Y. Payan, "In vivo measurement of human brain elasticity using a light aspiration device," *Medical Image Analysis*, vol. 13, no. 4, pp. 673–678, 2009.